MULTIPLICITY DISTRIBUTIONS IN K^+ Al AND K^+ Au COLLISIONS AT 250 GeV/c AND A TEST OF THE MULTIPLE COLLISION MODEL

EHS–NA22 Collaboration

Aachen[a]–Antwerp/Brussels[b]–Berlin(Zeuthen)[c]–Helsinki[d]– Krakow[e]–Moscow[f]–Nijmegen[g]–Rio de Janeiro[h]–Serpukhov[i]–Warsaw[j]–Yerevan[k]

I.V. AJINENKO[i], Yu.A. BELOKOPYTOV[i], H. BIALKOWSKA[j], H. BOETTCHER[c], P.V. CHLIAPNIKOV[i], F. CRIJNS[g], A. DE ROECK[b,1], E.A. DE WOLF[b,2], K. DZIUNIKOWSKA[e], A.M.F. ENDLER[h], A. ESKREYS[e], Z.C. GARUTCHAVA[i], Y. GOLUBKOV[f], H. GRAESSLER[a], G.R. GULKANYAN[k], P. van HAL[g,3], R.Sh. HAKOBYAN[k], T. HAUPT[g,4], W. KITTEL[g], D. KISIELEWSKA[e], B.B. LEVCHENKO[f], F. MEIJERS[g,5], A.B. MICHAŁOWSKA[b], Th. NAUMANN[c], V.I. NIKOLAENKO[i], K. OLKIEWICZ[e], B. PAWLIK[e], L.P. PETROVIKH[i], R. PÖLLÄNEN[d], V.M. RONJIN[i], A.M. RYBIN[i], H.M.T. SAARIKKO[d], W. SCHMITZ[a], L. SCHOLTEN[g], L.N. SMIRNOVA[f], O.G. TCHIKILEV[i], A.G. TOMARADZE[i,6], V.A. UVAROV[i], F. VERBEURE[b], R. WISCHNEWSKI[c],

(Submitted to Zeits. für Physik)

[a]III. Physikalisches Institut B, RWTH, D-5100 Aachen, Federal Republic of Germany (partially funded by the German Federal Minister for Research and Technology (BMFT) under the contract number 053AC41P)

[b]Inter-University Institute for High Energies, B-1050 Brussels and Dept. of Physics, Universitaire Instelling Antwerpen, B-2610 Wilrijk, Belgium

[c]Institut für Hochenergiephysik der Akademie der Wissenschaften der DDR, DDR-1615 Berlin-Zeuthen, German Democratic Republic

[d]Department of High Energy Physics, University of Helsinki, SF-00170 Helsinki, Finland

[e]Institute of Physics and Nuclear Techniques of the Academy of Mining and Metallurgy and Institute of Nuclear Physics, PL-30055 Krakow, Poland; partially supported by grants from CPBP 01.06 and 01.09

[f]Moscow State University, SU-119899 Moscow, USSR

[g]University of Nijmegen and NIKHEF-H, NL-6525 ED Nijmegen, The Netherlands

[h]Centro Brasileiro de Pesquisas Fisicas, Rio de Janeiro, Brazil

[i]Institute for High Energy Physics, SU-142284 Serpukhov, USSR

[j]University of Warsaw and Institute of Nuclear Problems, PL-00681 Warsaw, Poland; partially supported by grants from CPBP 01.06 and 01.09

[k]Institute of Physics, SU-375036 Yerevan, USSR

[1]Onderzoeker IIKW, Brussels, Belgium

[2]Bevoegdverklaard Navorser NFWO, Belgium

[3]Now with Ericsson Telecommunicatie B.V., Rijen, The Netherlands

[4]On leave from Institute of Nuclear Physics, Cracow, Poland

[5]Now at CERN, Geneva, Switserland

[6]Visitor from Institute of High Energy Physics of Tbilisi State University, USSR

Abstract

Multiplicity distributions, observed in K^+ interactions with Al and Au nuclei at 250 GeV/c incident momentum are presented. They are analyzed in the framework of multiple collisions of the incident particle inside a nucleus. The probability distribution of the number of grey tracks is well described by the model of Andersson et al., if a negative binomial distribution is assumed for the distribution of the number of grey protons produced per elementary collision instead of the usual geometrical distribution. The analysis of the average and dispersion of the charge multiplicity distribution supports the validity of the multiple collision model, including results on correlations between forward and backward average multiplicities.

1 Introduction

A detailed understanding of hadron interactions in nuclei is far from being achieved. The available experimental data either suffers from low statistics in bubble chamber experiments or from limited acceptance in counter experiments. The advent of experiments on nucleus-nucleus interactions demonstrates even more clearly the need for accurate data on hadron-nucleus collisions, as a reference frame for understanding the new data on heavy ion collisions.

Several experiments have yielded results on proton-nucleus collisions in the energy range of a few hundred GeV (See ref. [1] for a review). Furthermore, low statistics results have been published [2] on p Al and p Au interactions at 360 GeV/c in the same experimental set-up as used by us.

However, few experimental results are available on interactions of positive mesons with nuclei in this energy range. Multiplicity distributions in $\pi^{\pm}$, p and $\overline{p}$ interactions on Mg, Ag and Au at 100 GeV/c incident momentum are given in [3], again based on small statistics per channel. The same holds for [4] where π^+, K^+ and p interactions on Al and Au are studied at 200 GeV/c. Differential spectra for π^+ and K^+ interactions on various nuclei are presented in [5]–[7].

In this paper we present results from K^+ interactions on aluminum and gold nuclei at 250 GeV/c, the highest energy so far available for K^+ beams. The data are derived from a hybrid bubble chamber experiment and the statistics amounts to about thousand events per type of interaction.

In Section 2 we give details on the experiment and on the selection procedure and present the negative particle multiplicities. In Section 3 we discuss the number of grey particles and their connection with the number of collisions inside the nucleus. The dependence of the average multiplicity of negative particles and its dispersion on the number of collisions is analyzed in Section 4. Multiplicity correlations are discussed in Section 5. Our conclusions are summarized in Section 6.

2 Experimental Details

The data presented in this paper are obtained in the experiment NA22, performed at CERN with the European Hybrid Spectrometer (EHS). The Rapid Cycling Bubble Chamber (RCBC) with a diameter of 80 cm was filled with H_2 and used as a vertex detector. It was equipped with two nuclear targets, one of aluminum (mass number A=27) and one of gold (mass number A=197) of thickness 2.5 mm and 0.64 mm respectively (density of 0.68 and 1.24 g/cm^2 respectively) corresponding to 0.5% of an interaction length. The foils were placed side by side orthogonally to the beam, 15.5 cm behind the entrance window of the chamber. Charged tracks from nuclear interactions could thus be followed and measured in the hydrogen over a distance of maximally 65 cm.

The data were taken with a minimum bias interaction trigger described in [8], where the details of the experimental set-up and scanning procedures are given (see also [9]). In total 2900 K^+ events which are candidate interactions in the foils have been measured. Charged particle tracks are reconstructed from hits in the wire- and drift chambers of the EHS spectrometer and from tracks measured in the bubble chamber. The majority of protons with laboratory momentum less than 400 MeV/c stop inside the bubble chamber. The momentum of these tracks is accurately determined from their range in hydrogen. All reconstructed events were inspected on the scanning table and the ionization of positive tracks with laboratory momentum less than 1.2 GeV/c and of negative tracks with momentum less than 250 MeV/c was estimated visually. Low energy electrons and positrons from γ–conversions in the foils are identified. Positive tracks with momentum less than 1.2 GeV/c and with ionization compatible either uniquely with the p or with both the K and p hypotheses, are accepted as protons.

The event sample selected for this analysis satisfies the following criteria:

- the incident particle track is well measured and matches with the hits in the upstream wire chambers;
- the reconstructed vertex position is within one of the foils;
- the outgoing tracks are satisfactorily measured and reconstructed; the accepted loss of tracks due to measurement or reconstruction failures is at most one for charged multiplicities up to 10, and at most 20% for higher multiplicities;
- the event is not a candidate for a quasi-elastic or coherent interaction;
  - A quasi-elastic event is defined by the following criteria:
    1. the charge multiplicity equals two,
    2. the missing transverse momentum is less than 0.2 GeV/c,

3. the missing longitudinal momentum is less than 9 GeV/c.

– A coherent interaction is defined by the requirements that

1. the charge multiplicity is odd and ≤ 5,
2. all charged particles have rapidities larger than one, if measured in the K^+–nucleon c.m. system.

Among the accepted charged tracks remains a small admixture of unidentified electrons and positrons, arising from γ–conversions in the foils. It is estimated from the π^0 cross section and the thickness of the foils, to be of the order of 2% of all charged tracks in a K^+Al and 7% in a K^+Au event.

The loss of events, due to measurement or reconstruction failures or to the above selection criteria, is compensated by weighting the events with a multiplicity dependent correction factor, calculated as the ratio of the number of scanned to the number of accepted events. The number of accepted events amounts to 1082 K^+Al and 962 K^+Au interactions. The admixture of interactions in H_2 in this sample is estimated to be less than 4% in the Al and less than 2% in the Au sample. In the following the nuclear data will also be compared with K^+p data, obtained in the same experiment. For this comparison, elastic and single diffractive events are removed, according to cuts described in [9].

The multiplicity distribution of negative particles is shown in Fig. 1a for K^+ Al and in Fig. 1b for K^+ Au interactions. These, as well as the multiplicity distributions of all charged and of positive particles in both samples are fitted with the Negative Binomial Distribution (NBD):

$$P(n) = \left(\begin{array}{c} n+k-1 \\ n \end{array} \right) \left(\frac{\frac{\overline{n}}{k}}{1+\frac{\overline{n}}{k}} \right)^n \left(\frac{1}{1+\frac{\overline{n}}{k}} \right)^k \qquad (2.1)$$

The values of the average charge multiplicity $< n >$ and dispersion D, as well as the fitted parameters $\overline{n}$ and $1/k$ and the χ^2/NDF of the fits are collected in Table I. The fits are very good for negative particles (corresponding to produced particles), but less so for positive particles. The parameter $1/k$ for negative particles, which is a measure of the width of the multiplicity distribution, increases from zero in K^+p interactions[1] [10] to 0.117±0.013 for K^+ Al and 0.236±0.017 for K^+ Au interactions. This indicates a significant broadening of the multiplicity distribution for heavier nuclei. The rapidity dependence of NBD fits will be presented in a forthcoming analysis.

[1]It was checked that the $1/k$ value cited in ref. [10] for π^+p is the same for K^+p interactions

3 Distribution of "Grey" Protons and the Number of Projectile Collisions inside the Nucleus

Most models for hadron-nucleus collisions are based on the hypothesis of multiple independent collisions of the projectile or its constituents with the nucleons of the target nucleus [1]. In these models the incident hadron may interact once or several times with the target nucleons depending on the impact parameter of the hadron and on the size of the nucleus. The struck nucleons recoil and either leave the target nucleus or scatter with other target nucleons, yielding second generation nucleons, which can again collide to produce a third generation and so on. For a given nucleus, one can estimate the average number of projectile collisions $\overline{\nu}_A$ from the relation [11]

$$\overline{\nu}_A = \frac{A \cdot \sigma_{hN}}{\sigma_{hA}} \tag{3.1}$$

where σ_{hN} and σ_{hA} are the cross sections for hadron h interacting with a nucleon N or a nucleus of atomic number A, respectively. The actual number of collisions ν is assumed to be statistically correlated with the number of protons knocked out of the nucleus, either in the interaction of the projectile with the target nucleons or in the collisions of secondary particles coming from the intranuclear cascade. All protons with kinetic energy between $\sim$ 30 and $\sim$ 400 MeV are considered to be originating from such an intranuclear cascade. All these protons fall into the class of grey tracks, defined by the velocity interval $0.2 < \beta < 0.7$ or equivalently a momentum interval of 190 to 920 MeV/c, according to the nomenclature used in emulsion experiments. Less energetic protons, observed in emulsions as black tracks, are mostly associated with the evaporation of the nucleus and are subject to sizable losses in our experimental conditions. For more energetic protons, the visual identification becomes gradually more uncertain with increasing momentum. We denote the number of grey protons in an event by n_g.

The laboratory momentum spectrum of identified protons for both the K^+ Al and K^+ Au data combined, is shown in Fig. 2, where also the range of protons accepted as grey tracks is indicated. The average number of grey tracks amounts to 1.08±0.04 in K^+ Al and 3.38±0.12 in K^+ Au events. The loss of low energy protons (p_{lab} <450 MeV/c) which are slowed down to a momentum p_{lab} <200 MeV/c or absorbed in the foils or stopped in the adjacent volume of the liquid hydrogen, is estimated to be less than 17%.

Several models have been proposed to express the correlation between the number of grey protons and the number of projectile collisions in a quantitative way [12,13]. In our analysis we use the method proposed by Andersson et al. [12]. According to this model the probability of observing n_g grey protons in an event with ν collisions

of the projectile inside a nucleus with atomic number A is given by

$$P_\nu^A(n_g) = \left(\begin{array}{c} n_g + \nu - 1 \\ n_g \end{array} \right) (1-x)^\nu x^{n_g} \tag{3.2}$$

with

$$x = (\overline{n}_g/\overline{\nu})/(1+\overline{n}_g/\overline{\nu}) \tag{3.3}$$

if one assumes the geometrical distribution (GD) of n_g *for a single collision* as in the original paper of Andersson et al [12].

Summing over all numbers of collisions ν, one obtains as a probability for n_g grey tracks in an event:

$$P^A(n_g) = \sum_{\nu=1}^{A} \Pi_A(\nu).P_\nu^A(n_g) \tag{3.4}$$

where $\Pi_A(\nu)$ is the probability distribution of ν. The latter can be calculated in the Glauber model [14] using the total inelastic cross section and the nuclear size.

However, for heavy nuclei a disagreement of the predicted $P^A(n_g)$ with the experimental data is observed. Since the Negative Binomial Distribution (NBD) has been very succesfull in describing multiplicity distributions of produced particles, it is tempting to try it also for the distribution of grey particles in a single collision. The NBD function contains a parameter k which is obtained by a fit to the n_g distribution and which may depend on the atomic mass number A. This corresponds to allowing not only the average multiplicity of grey tracks to change with A, but also the dispersion of the distribution and therefore a better agreement with the data may be expected. (Note that the GD can be considered as a particular case of the NBD with k=1). In this case the formulae (3.2) and (3.3) are replaced by

$$P_\nu^A(n_g) = \left(\begin{array}{c} n_g + k\nu - 1 \\ n_g \end{array} \right) (1-x)^{k\nu} \cdot x^{n_g} \tag{3.5}$$

with

$$x = \left(\frac{\overline{n}_g}{k\overline{\nu}}\right) / \left(1 + \frac{\overline{n}_g}{k\overline{\nu}}\right) \tag{3.6}$$

The function $P_\nu^A(n_g)$ is shown in Figs. 3a and 3b, superimposed on the experimental n_g distributions obtained for aluminum and gold. The fitted values of the parameter k are 1.5±0.1 for K^+ Al and 0.5±0.02 for K^+ Au . Both cases discussed above, i.e. GD and NBD of the number of grey protons in a single collision, are considered. For aluminum hardly any difference is observed between the GD and the NBD and therefore only one curve is shown. For gold, however, the agreement with the data improves considerably by using the NBD. Of course we should keep in mind that an additional free parameter has been introduced.

4 Dependence of the Multiplicity Distribution on the Number of Projectile Collisions

In this section we analyse the dependence of the multiplicity distribution of the negative particles on the average number of projectile collisions $\overline{\nu}$. We limit the analysis to negative particles since they are pions to a good approximation, while positive particles contain a sizable contribution of unidentified protons and kaons with momenta above 1.2 GeV/c.

The overall multiplication of particle production in an interaction with a nucleus is measured by the ratio $R = \overline{n}_{hA}/\overline{n}_{hp}$ and depends on the number of projectile collisions $\overline{\nu}$. The dependence of R on $\overline{\nu}(n_g)$ for negative particles is shown in Fig. 4, together with the values for the full samples (the open symbols, indicated by arrows). In this figure and in the following one, a data point is given for each value of n_g, starting from n_g=0 up to 6 for K^+ Al and up to 17 for K^+ Au . As observed before [15], the relation between R and $\overline{\nu}(n_g)$ is linear and has the same slope of 0.5 as R vs. ν_A for the full samples on different nuclei.

As shown in Figs. 5a,b the dispersion D of the distribution of the number of produced negative particles increases with $\overline{\nu}(n_g)$, while $D/\overline{n}$ decreases with $\overline{\nu}(n_g)$. This confirms earlier observations made in [15] and [16].

Using the approach of Andersson et al. [12] or Hegab and Hüfner [13], one can find the average $\overline{\nu}(n_g)$ and the variance $D^2_\nu(n_g)$ of the number of collisions for each subsample with fixed number n_g of grey protons. For $\overline{\nu}(n_g)$ one obtains

$$\overline{\nu}(n_g) = \left(\sum_\nu \Pi_A(\nu) \cdot \nu P^A_\nu(n_g)\right) / P^A(n_g) \tag{4.1}$$

It should be stated clearly that the estimation of $\overline{\nu}$ for a given n_g is not unique. As demonstrated in Figs. 6 and 7, one obtains different results for the average and the dispersion of the number of collisions by using different models as e.g. [12] and [13], and by using either the GD or the NBD for the n_g distribution in a single collision. This holds particularly for the heavier nuclei such as gold, where 20% of the interactions have 6 or more grey protons and where $\overline{\nu}(n_g)$ and particularly the dispersion are very different for the various models at large n_g.

Here we use the method of Andersson et al. with a NBD for n_g, since this reproduces the experimental distribution of grey protons $P^A_{\rm exp}(n_g)$ very well (see Fig. 3). This agreement is essential in order to reproduce the average number of collisions given by the Glauber model as the average value over $P^A_{\rm exp}(n_g)$ calculated as

$$\overline{\nu} = \sum_{n_g} P^A_{\rm exp}(n_g)\overline{\nu}(n_g)$$

and found to be 1.67 and 2.61 for K^+ Al and K^+ Au respectively, in agreement with the values 1.64 and 2.55, calculated with (3.1).

For a more differential analysis we have divided the samples of interactions with aluminum and gold into subsamples of fixed number of grey protons. Small subsamples with large numbers of grey protons are combined in order to obtain reasonable statistics. The subsamples used are defined in the first column of Table II, the values obtained for $\overline{\nu}$ and D^2_ν are given in columns 2 and 3. In this way, we are able to study interactions with on average more than four collisions per interaction instead of 2.6 collisions on gold. Our results in Table II confirm earlier observations that the average number of collisions $\overline{\nu}$, its variance D^2_ν, the average negative multiplicity $\overline{n}$ and its variance $D^2_{\rm exp}$ are all rising functions of the number of grey particles.

The dependence of the average number of negative particles $\overline{n}$ and its variance D^2 on $\overline{\nu}$ can be further investigated in terms of particular models. Here we test a simple multiple collision model [17, 18] in which the following assumptions are made:

- the first collision is the same as scattering on a free nucleon with average multiplicity $\overline{n}^0$ and variance $D^2_{n^0}$;
- each next collision leads on average to the production of $\overline{n}^i$ particles with variance $D^2_{n^i}$.

The average multiplicity is then

$$\overline{n} = \overline{n}^0 + (\overline{\nu} - 1)\overline{n}^i \tag{4.2}$$

and the variance

$$D^2_n = \mathrm{var}(n) = \overline{n^2} - \overline{n}^2 = D^2_{n^0} + (\overline{\nu} - 1)D^2_{n^i} + (\overline{n}^i)^2 D^2_\nu \tag{4.3}$$

with

$$D^2_\nu = \overline{\nu^2} - \overline{\nu}^2 \tag{4.4}$$

where D^2_n, D^2_ν, $D^2_{n^0}$ and $D^2_{n^i}$ represent the variances of the distributions of n, ν, n^0 and n^i, respectively.

Measurements of $\overline{n}$ and D^2_n for the two nuclei provide the information necessary to calculate the unknown values of $\overline{n}^0$, $D^2_{n^0}$, $\overline{n}^i$ and $D^2_{n^i}$. Assuming 4.2 – 4.4 to hold for all subsamples with fixed number of grey protons, we use the measurements $\overline{n}_{\rm exp}$ and $D^2_{\rm exp}$ for the five subsamples defined in Table II and obtain an overdetermined set of equations which is solved by the least squares method. The fit results are given at the top of Table II. In columns 5 and 7 of Table II we also show the $\overline{n}_{\rm fit}$ and $D^2_{\rm fit}$ calculated for each subsample from the fitted parameters. The overall agreement between the experimental and fitted values of $\overline{n}$ and D^2 for each of the various classes is very good. Moreover, the fitted values of $\overline{n}^0$ and $D^2_{n^0}$ are in fair agreement with

what they should correspond to, that is the values of the average negative multiplicity and variance for K^+ collisions on a free proton, found to be 3.45±0.01 and 3.46±0.06. The latter values are obtained by imposing the same selection criteria on our K^+p sample. From Table II we note that the first collision in the nucleus is about twice as efficient in producing particles than each of the next collisions.

In conclusion we observe that this simple model of multiple collisions works remarkably well, if the first two moments of the negative multiplicity distributions are considered.

5 Multiplicity Correlations

A further test of the simple model of multiple collisions used above, can be supplied by a study of the correlations between the multiplicities, observed in different kinematical regions [18]. Again, the discussion is limited to negative particles only and we consider them to be pions.

To define a kinematical region we use the rapidity variable y calculated in the c.m. system for a collision of the incident K^+ with a nucleon at rest. We analyze the multiplicity correlations observed between the two rapidity regions $y \in (-2.5, -0.5)$, called "left" (L) and $y \in (-0.5, 1.5)$ called "right" (R). These kinematical regions are chosen in order to minimize correlations due to energy-momentum conservation (in the very forward region) and to the process of cascading (in the very backward region).

We would like to check if the correlation between multiplicities in these two kinematical regions follows the pattern expected from the multiple collision model [18]. Assuming that the model can be applied in restricted rapidity intervals, the formulae (4.2) and (4.3) are valid for the regions R and L separately and the fits of $\overline{n}^0$, $\overline{n}^i$, $D^2_{n^0}$ and $D^2_{n^i}$ can be repeated in each of these regions. The results for the previously defined subsamples of fixed n_g are listed in Tables III and IV, and shown in Figs. 8a,b. The open triangle (circle) pertains to the full sample of K^+ Al (K^+ Au) interactions.

The linearity of the dependence of $\overline{n}_L$ and $\overline{n}_R$ on $\overline{\nu}(n_g)$ is still preserved[2], and the agreement between the experiment and the model remains good (see Tables III and IV).

As a measure of the correlation we use the covariance D^2_{LR}

$$D^2_{LR} = \overline{n_R \cdot n_L} - \overline{n}_R \cdot \overline{n}_L = \mathrm{cov}(\overline{n}_R \cdot \overline{n}_L) = \frac{1}{2}\left(D^2_n - D^2_{n_R} - D^2_{n_L}\right) \quad . \tag{5.1}$$

It is easy to show that, using 4.2 and 4.3 in each region, one arrives at the expression

$$D^2_{LR} = \left(D^{n^0}_{LR}\right)^2 + \overline{n}^i_R \cdot \overline{n}^i_L \cdot D^2_\nu + (\overline{\nu} - 1)\left(D^{n^i}_{LR}\right)^2 \tag{5.2}$$

where $\left(D^{n^0}_{LR}\right)^2$ and $\left(D^{n^i}_{LR}\right)^2$ are the covariances of the n^0 and n^i distributions in the two regions. Again, using the seven subsamples of fixed n_g, one can fit the two covariances and the results are shown in Table V. It is seen that the experimental and fitted covariances agree very well.

In formula 5.2 both the long range correlations induced by the spread of the number of collisions ν in the sample and the short range correlations (string effects)

[2]The fact that the fitted value of $\overline{n}_R$ at $\overline{\nu}$=1, i.e. 1.9, does not coincide with the corresponding value observed in K^+p interactions [9], should not be surprising, if one considers the different meaning of the "same"rapidity intervals in K^+p and K^+ nucleus collisions.

are taken into account. If the short range contribution can be neglected both $\left(D^{n^0}_{LR}\right)^2$ and $\left(D^{n^i}_{LR}\right)^2$ should vanish. This is expected from the observation made in elementary K^+p collisions where the $\pi^-\pi^-$ short range correlations are very weak [19]. Within two standard deviations, both values are indeed consistent with zero. Thus D^2_{LR} is simply proportional to D^2_ν with a coefficient expected by the model.

A more widely accepted approach in similar studies is to discuss the relation between $\overline{n}_L$ and n_R or vice versa:

$$\overline{n}_L = b_L n_R + a_L \tag{5.3}$$

In this approach b_L measures the strength of the correlation. The value of b_L is connected with the quantities used in our analysis by the relation

$$b_L = \frac{D^2_{LR}}{D^2_{nR}} = \frac{\overline{n}^i_R \cdot \overline{n}^i_L \cdot D^2_\nu}{D^2_{n^0_R} + (\nu - 1)D^2_{n^i_R} + \overline{n}^i_R D^2_\nu} \tag{5.4}$$

It was shown in the experiment NA5 [20] that the correlation strength increases with increasing D^2_ν as expected.

We thus confirm that the model of independent projectile collisions works well, also when multiplicity correlation data are included.

6 Summary

We have performed an analysis of multiplicity distributions and multiplicity correlations on K^+ interactions with Al and Au nuclei, obtained in an EHS experiment at 250 GeV/c beam momentum. The analysis was made in terms of a simple approach, based on the assumption of multiple collisions of the incident particle inside a nucleus.

For the Au target, the distribution of the number n_g of grey protons is much better described in the framework of the Andersson et al. model, if one assumes a Negative Binomial Distribution for the number of grey particles produced in a single collision instead of the geometrical distribution.

We confirm that the average multiplicity of particles, as well as the dispersion of the distribution, are linearly increasing with the average number of collisions, if the sample is subdivided according to different numbers of n_g. The ratio $D/\overline{n}$ however is constant or slightly decreasing with $\overline{\nu}(n_g)$.

We show that the basic assumptions of the simple model of multiple collisions are correct if averages and dispersions are considered. Our analysis is extended to also include correlation results and agreement with this simple model is maintained.

Acknowledgements

We are deeply indebted to the CERN SPS, beam and EHS crews for their support during preparation and runs of our experiment. It is a pleasure to thank the scanning and measuring staffs of our laboratories for their tedious effort in scanning and measuring these, often very complicated, events.

7 References

1. S. Frederiksson, G. Eilam, G. Berlad and L. Bergström, Phys. Reports **144** (1987) 188
2. J.L. Bailly et al., Z. Phys. **C35** (1987) 301
3. N.N. Biswas et al., Phys. Rev. **D33** (1986) 3167
4. D. Brick et al., Nucl. Phys. **B201** (1982) 189
5. J. Elias et al., Phys. Rev. **D22** (1980) 13
6. D. Barton et al., Phys. Rev. **D27** (1983) 2580
7. K. Braune et al., Z. Phys. **C13** (1982) 191
8. NA22 Collaboration: M. Adamus et al., Z. Phys. **C32** (1986) 475
9. NA22 Collaboration: M. Adamus et al., Z. Phys. **C39** (1988) 311
10. NA22 Collaboration: M. Adamus et al., Z. Phys. **C37** (1988) 215
11. A. Białas and W. Czyż, Phys. Lett. **51B** (1974) 179. and W. Busza et al., Phys. Rev. Lett. **34** (1975) 836
12. B. Andersson, I. Otterlund and E. Stenlund, Phys. Lett. **73B** (1978) 343
13. M.K. Hegab and J. Hüfner, Nucl. Phys. **A384** (1982) 353
14. R.J. Glauber and G. Mathiae, Nucl. Phys. **B21** (1970) 135
15. C. de Marzo et al., Phys. Rev. **D29** (1984) 2476
16. S.A. Azimov et al., Sov. J. Nucl. Phys. **33** (1981) 169
17. J. Hüfner and B. Liu, Z. Phys. **C27** (1985) 283
18. K. Fiałkowski, Acta Phys. Pol. **B17** (1986) 623
19. NA22 Collaboration: V.V. Aivazyan et al., *Forward-Backward multiplicity correlations in K^+p and pp collisions at 250 GeV/c*, preprint HEN-308/1988, University of Nijmegen preprint
20. I. Derado et al., Z. Phys. **C40** (1988) 25

8 Figure Captions

1. Multiplicity distributions of negative particles and NBD fits for a) K^+ Al and b) K^+ Au .

2. Momentum spectrum of all identified protons in the combined K^+ Al and K^+ Au samples. The velocity interval $0.2 < \beta < 0.7$ is used to define the grey protons and is marked by arrows.

3. Probability $P(n_g)$ for producing n_g grey protons in a) K^+ Al and b) K^+ Au collisions. The curves are calculated from eq. (3.2) using the GD (Geometrical Distribution) and (3.5) using the NBD (Negative Binomial Distribution) for n_g in a single collision.

4. The ratio $R = \overline{n}_{K^+A}/\overline{n}_{K^+p}$ for negative particles versus the average number $\overline{\nu}(n_g)$ of projectile collisions for K^+ Al (triangles) and K^+ Au (circles). The ratios obtained for the full samples of Al and Au are marked by arrows. Each data point corresponds to a given n_g. A line of the form $R = 0.5(\overline{\nu}(n_g) + 1)$ is shown for comparison.

5. a) Dispersion D versus $\overline{\nu}(n_g)$ and b) $D/\overline{n}$ versus $\overline{\nu}(n_g)$. Data for K^+ Al and K^+ Au reactions are shown by triangles and circles, respectively.

6. Comparison of the dependence of the average number of collisions $\overline{\nu}(n_g)$ on n_g for K^+ Au interactions, calculated using different methods: Andersson et al. with the GD and with the NBD, and Hegab and Hüfner.

7. The dispersion squared in the number of collisions versus n_g for the same cases as in Fig. 4.

8. a) $\overline{n}_R$ and b) $\overline{n}_L$ versus $\overline{\nu}$. The data for K^+ Al and K^+ Au reactions are given by triangles and circles respectively. The lines are fits to eq. (4.2). The points indicated by arrows pertain to the full samples of K^+ Al and K^+ Au interactions.

Table I: Average multiplicities and dispersion of the multiplicity distributions for all particles, positives and negatives in K^+ Al and K^+ Au interactions. The fitted values of the parameters $\overline{n}_{\rm NBD}$ and $1/k$, and the χ^2/NDF of the NBD fit are also given.

		$\overline{n}$	D	$\overline{n}_{\rm NBD}$	$1/k$	χ^2/NDF
Al	all charged	13.11±0.18	6.61±0.15	13.02±0.18	0.115±0.009	27/32
	positives	8.10±0.11	4.01±0.09	8.15±0.10	0.079±0.007	47/22
	negatives	5.01±0.08	2.86±0.07	4.99±0.08	0.117±0.013	6/15
Au	all charged	20.13±0.38	12.69±0.32	19.52±0.38	0.284±0.011	63/60
	positives	13.42±0.27	9.12±0.24	13.79±0.24	0.234±0.011	116/42
	negatives	6.71±0.12	4.11±0.10	6.70±0.13	0.236±0.017	7/22

Table II: Fitted values of the average negative multiplicity and dispersion in the first and in later interactions. The various subsamples are also defined and the relevant quantities are shown for each subsample.

$\overline{n}^0$=3.73±0.28	$D^2_{n^0}$=4.45±0.11
$\overline{n}^i$=1.85±0.12	$D^2_{n^i}$=1.09±0.15

Sample	$\overline{\nu}$	D^2_ν	$\overline{n}_{\rm exp}$	$\overline{n}_{\rm fit}$	$D^2_{\rm exp}$	$D^2_{\rm fit}$
1) Al, $n_g \leq 1$	1.43	0.54	4.63±0.09	4.52	7.24±0.43	6.76
2) Al, $n_g \geq 2$	2.24	1.44	6.03±0.16	6.02	9.30±0.92	10.69
3) Al, all n_g	1.67	0.95	5.01±0.08	4.97	8.18±0.40	8.41
4) Au, $n_g \leq 1$	1.80	1.18	4.80±0.13	5.20	8.58±0.70	9.36
5) Au, $2 \leq n \leq 6$	2.91	2.42	7.25±0.19	7.25	14.75±1.38	14.82
6) Au, $n_g \geq 7$	4.13	3.48	10.30±0.30	9.51	18.92±2.52	19.71
7) Au, all n_g	2.61	2.77	6.71±0.12	6.71	16.89±0.82	15.68

Table III: Same quantities as in Table II for the "right region", as defined in the text.

$\overline{n}_R^0$=1.91±0.06	$D^2_{n_R^0}$=2.75±0.10
$\overline{n}_R^i$=0.33±0.06	$D^2_{n_R^i}$=0.24±0.06

Sample	$\overline{n}_{R(\text{exp})}$	$\overline{n}_{R(\text{fit})}$	D^2_{exp}	D^2_{fit}
1) Al, $n_g \leq 1$	2.10±0.06	2.05	2.99±0.17	2.92
2) Al, $n_g \geq 2$	2.25±0.09	2.32	3.24±0.32	3.20
3) Al, all n_g	2.14±0.05	2.13	3.06±0.14	3.03
4) Au, $n_g \leq 1$	2.07±0.08	2.17	2.86±0.24	3.06
5) Au, $2 \leq n \leq 6$	2.60±0.09	2.54	3.31±0.29	3.50
6) Au, $n_g \geq 7$	3.00±0.15	2.95	4.37±0.54	3.88
7) Au, all n_g	2.43±0.06	2.44	3.42±0.19	3.46

Table IV: Same quantities as in Table III for the "left region", as defined in the text.

$\overline{n}_L^0$=1.07±0.09	$D^2_{n_L^0}$=1.39±0.10
$\overline{n}_L^i$=1.09±0.05	$D^2_{n_L^i}$=0.75±0.11

Sample	$\overline{n}_{L(\text{exp})}$	$\overline{n}_{L(\text{fit})}$	D^2_{exp}	D^2_{fit}
1) Al, $n_g \leq 1$	1.60±0.05	1.54	2.53±0.16	2.37
2) Al, $n_g \geq 2$	2.45±0.11	2.42	4.04±0.40	4.04
3) Al, all n_g	1.83±0.05	1.80	3.10±0.14	3.03
4) Au, $n_g \leq 1$	1.74±0.07	1.94	2.72±0.23	3.39
5) Au, $2 \leq n \leq 6$	3.14±0.12	3.15	5.95±0.59	5.71
6) Au, $n_g \geq 7$	4.75±0.20	4.48	8.01±1.08	7.90
7) Au, all n_g	2.80±0.07	2.83	6.10±0.35	5.90

Table V: Left-right covariances for the full sample in the first and subsequent collisions and experimental and fitted covariances in the different subsamples.

$\left(D^{n^0}_{LR}\right)^2$ =0.17±0.08
$\left(D^{n^i}_{LR}\right)^2$ =0.06±0.08

Sample	$D^2_{LR(\mathrm{exp})}$	$D^2_{LR(\mathrm{fit})}$
1) Al, $n_g \leq 1$	0.41±0.08	0.39
2) Al, $n_g \geq 2$	0.68±0.17	0.77
3) Al, all n_g	0.51±0.08	0.55
4) Au, $n_g \leq 1$	0.69±0.11	0.65
5) Au, $2 \leq n \leq 6$	1.21±0.28	1.17
6) Au, $n_g \geq 7$	1.46±0.39	1.63
7) Au, all n_g	1.43±0.12	1.27

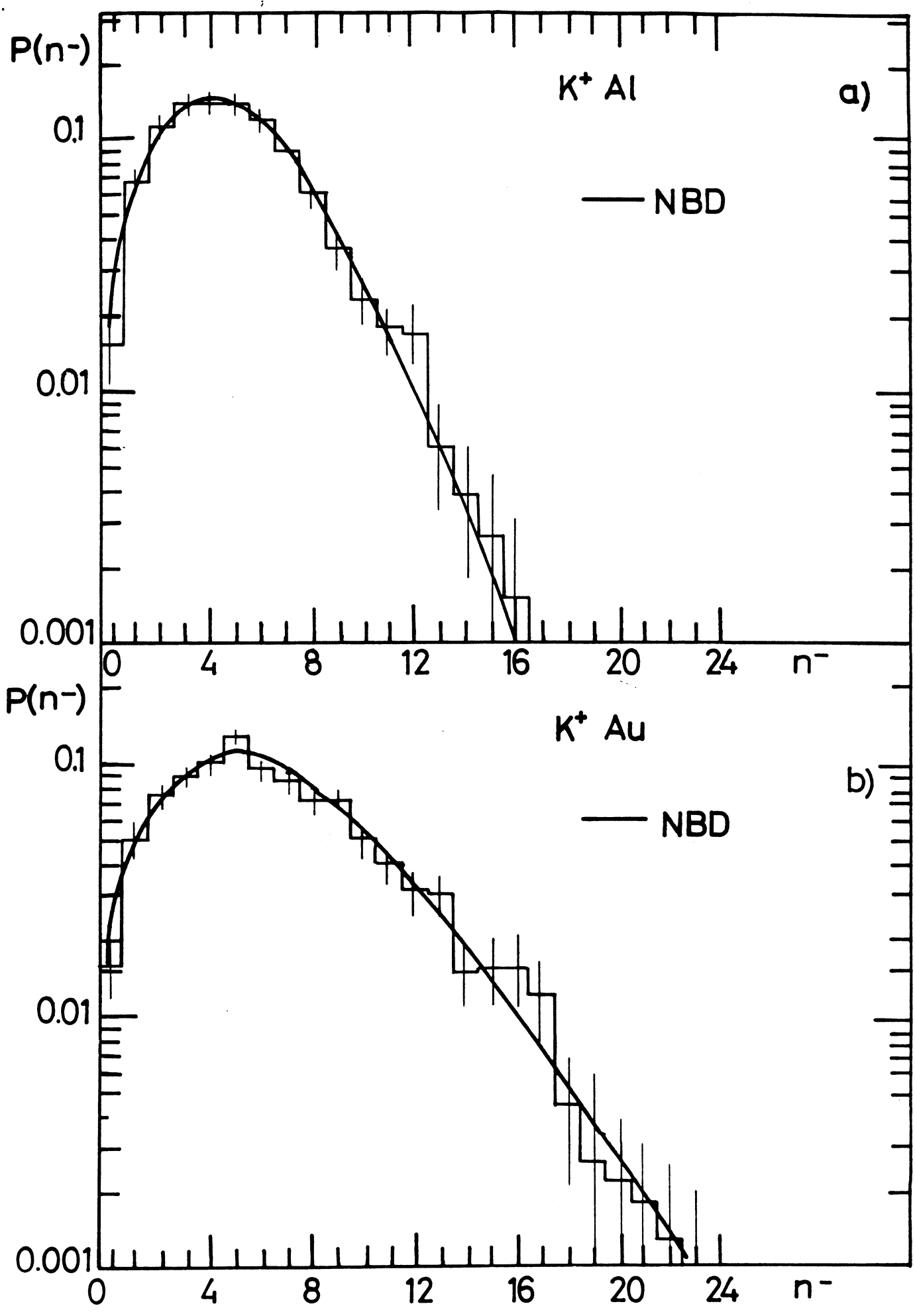
P(n⁻)
K⁺ Al
a)
NBD
0.1
0.01
0.001
0
4
8
12
16
20
24
n⁻
P(n⁻)
K⁺ Au
b)
NBD
0.1
0.01
0.001
0
4
8
12
16
20
24
n⁻

FIG. 1

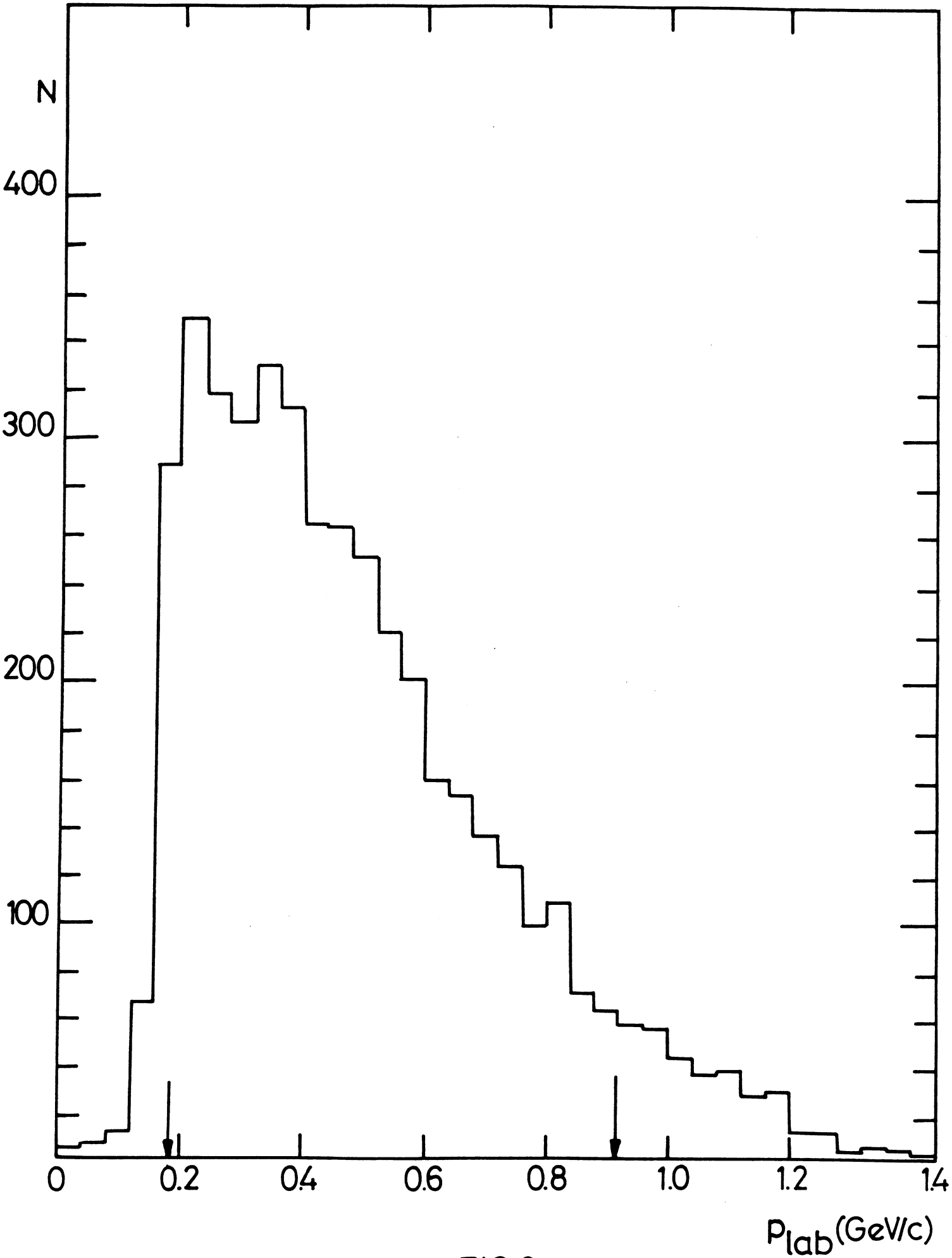

FIG.2

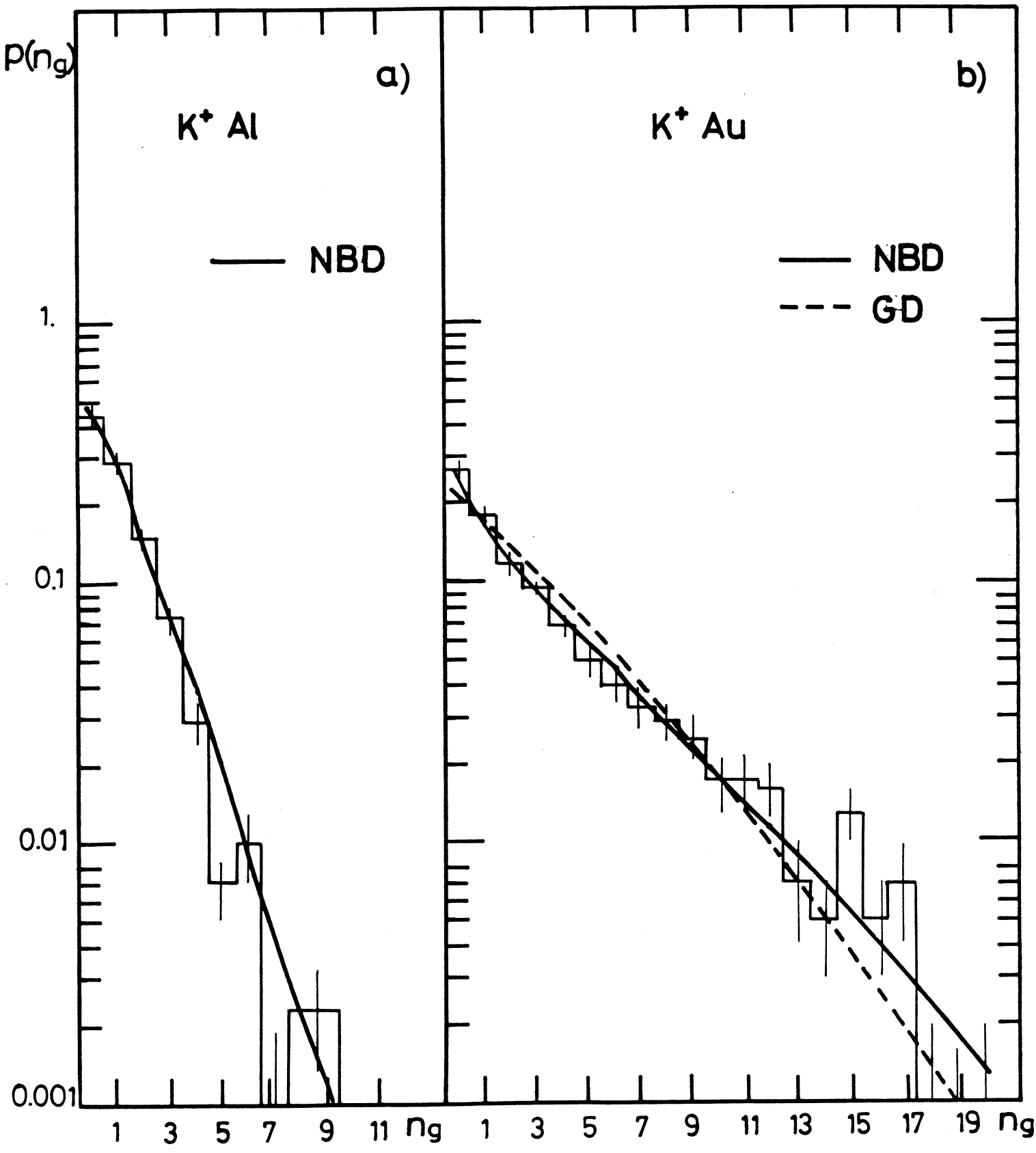
P(ng)
a)
K+ Al
NBD
b)
K+ Au
NBD
GD
1.
0.1
0.01
0.001
1 3 5 7 9 11 ng
1 3 5 7 9 11 13 15 17 19 ng

FIG. 3

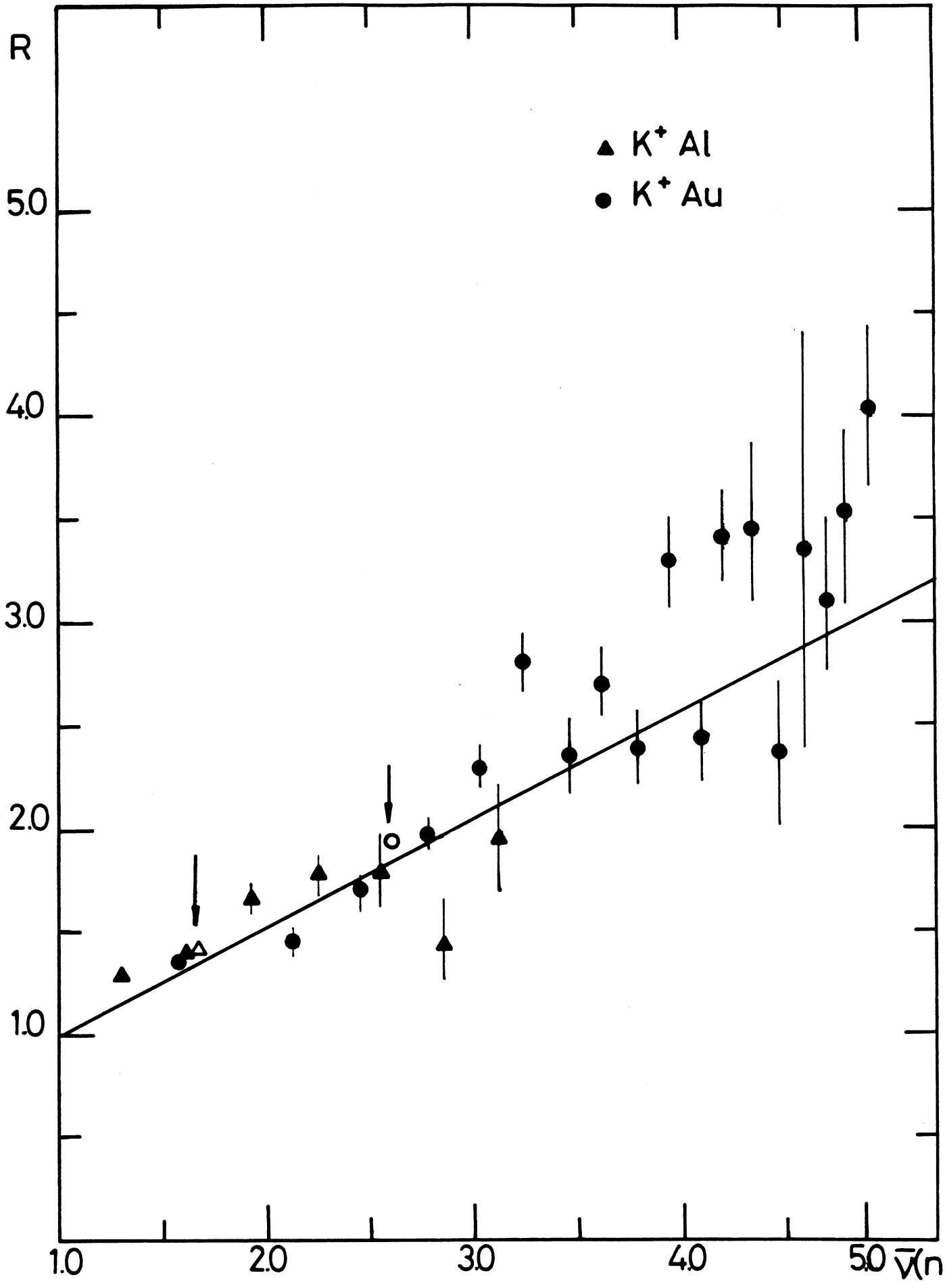

FIG. 4

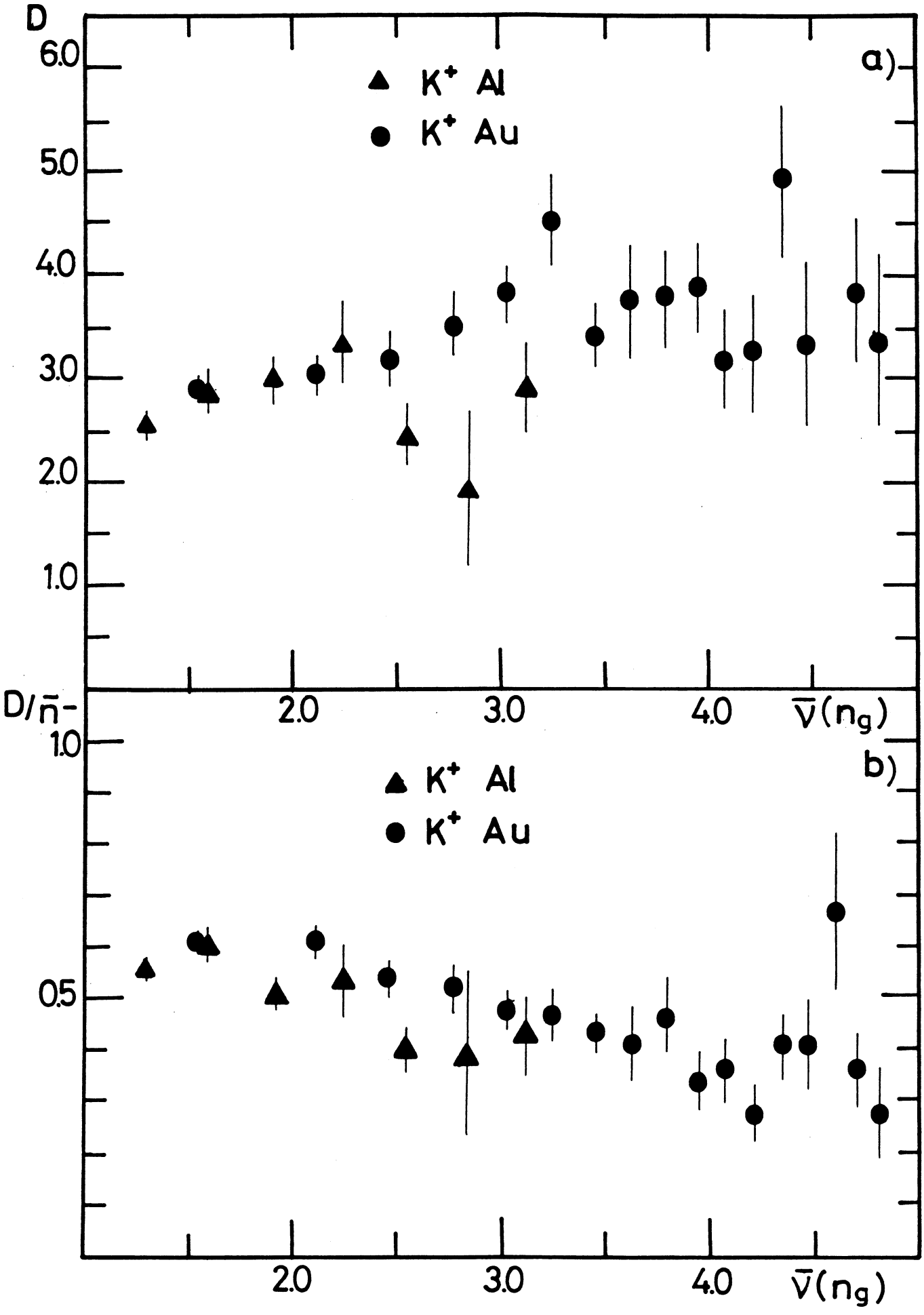
D
6.0
5.0
4.0
3.0
2.0
1.0
a)
▲ K+ Al
● K+ Au
2.0
3.0
4.0
ν̄(ng)
D/n̄ -
1.0
0.5
b)
▲ K+ Al
● K+ Au
2.0
3.0
4.0
ν̄(ng)

FIG. 5

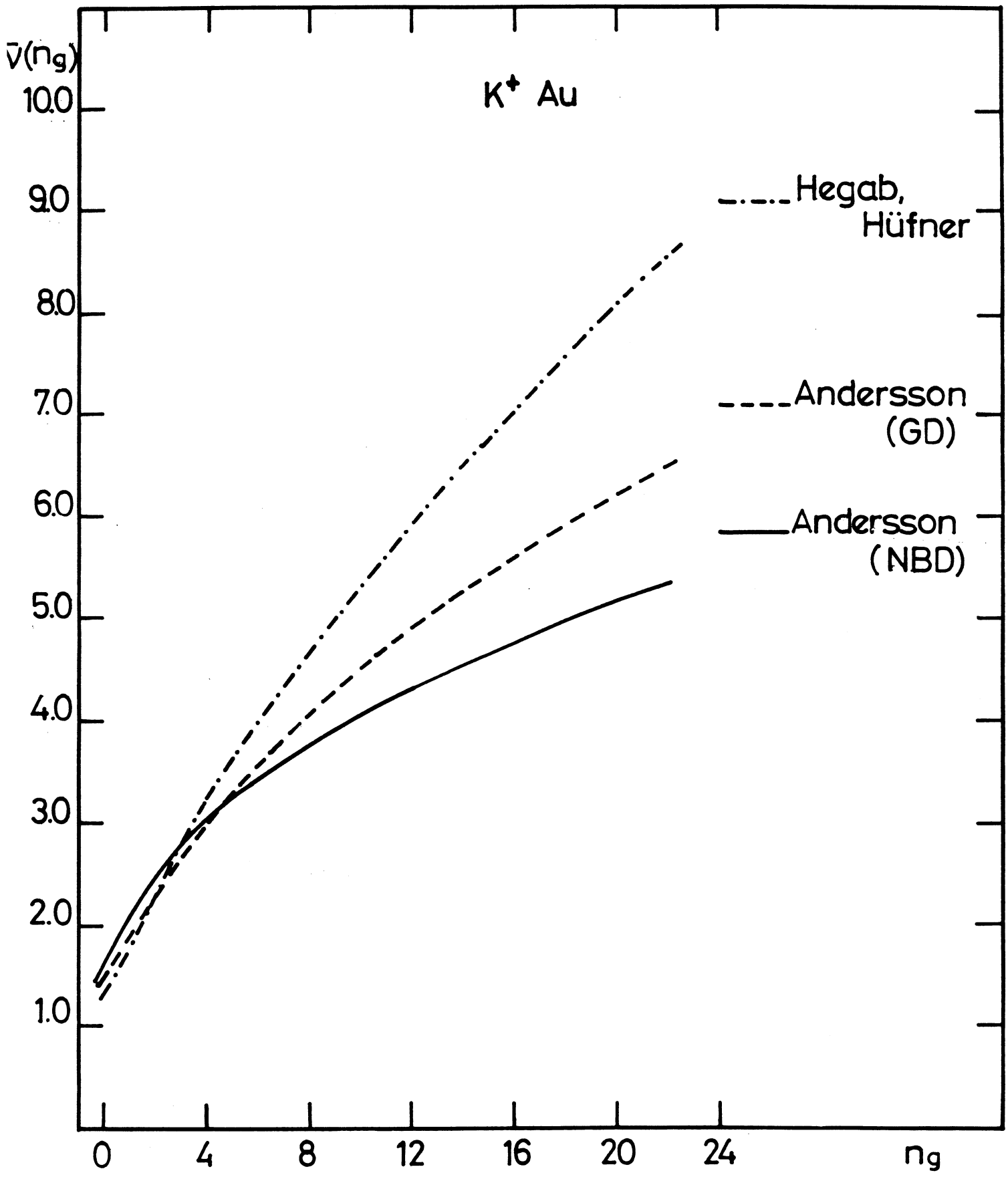
$\bar{\nu}(n_g)$
10.0
9.0
8.0
7.0
6.0
5.0
4.0
3.0
2.0
1.0
K^+ Au
Hegab, Hüfner
Andersson (GD)
Andersson (NBD)
0
4
8
12
16
20
24
n_g

FIG. 6

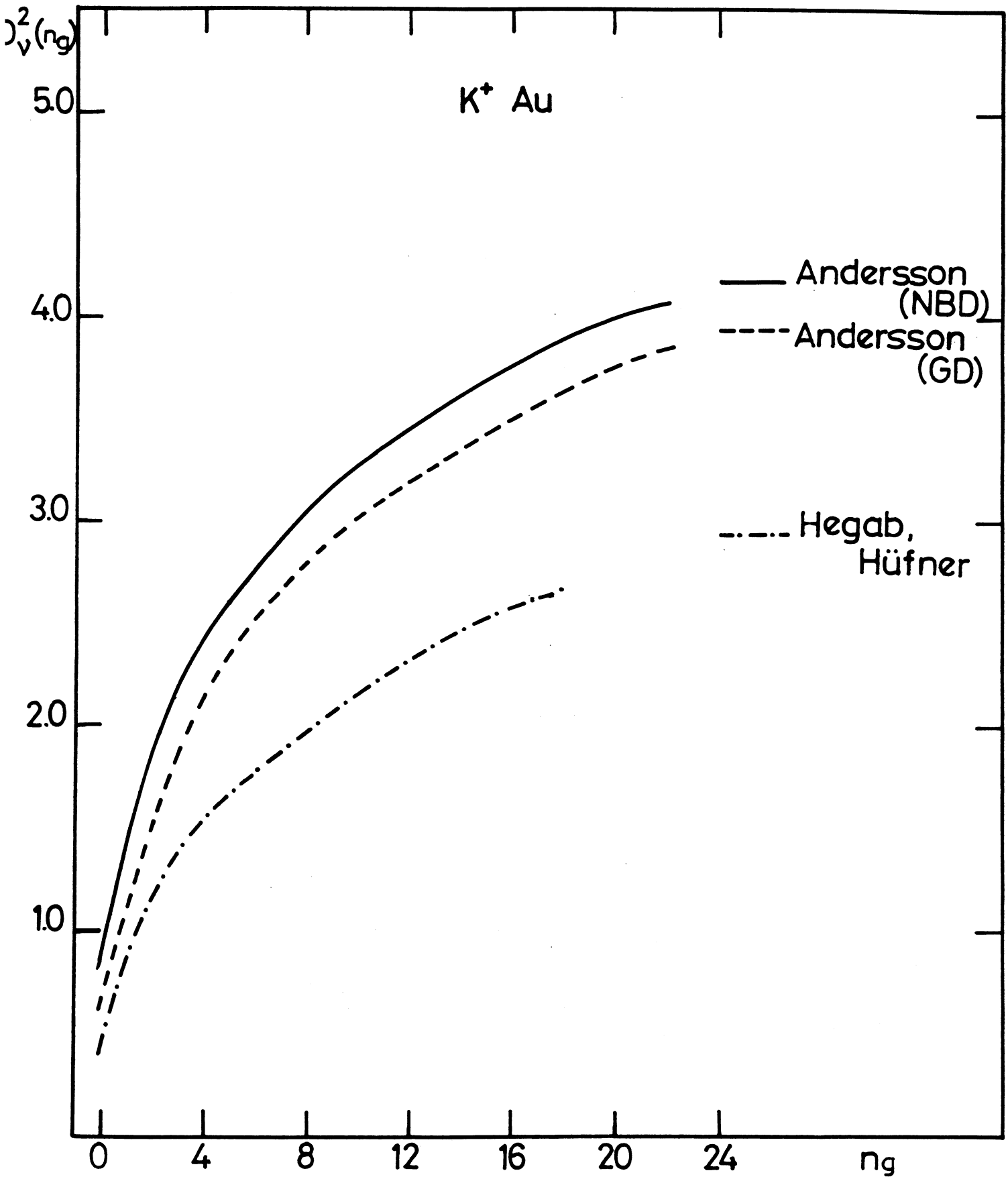
$D_\nu^2(n_g)$
5.0
4.0
3.0
2.0
1.0
K⁺ Au
Andersson (NBD)
Andersson (GD)
Hegab, Hüfner
0
4
8
12
16
20
24
n_g

FIG. 7

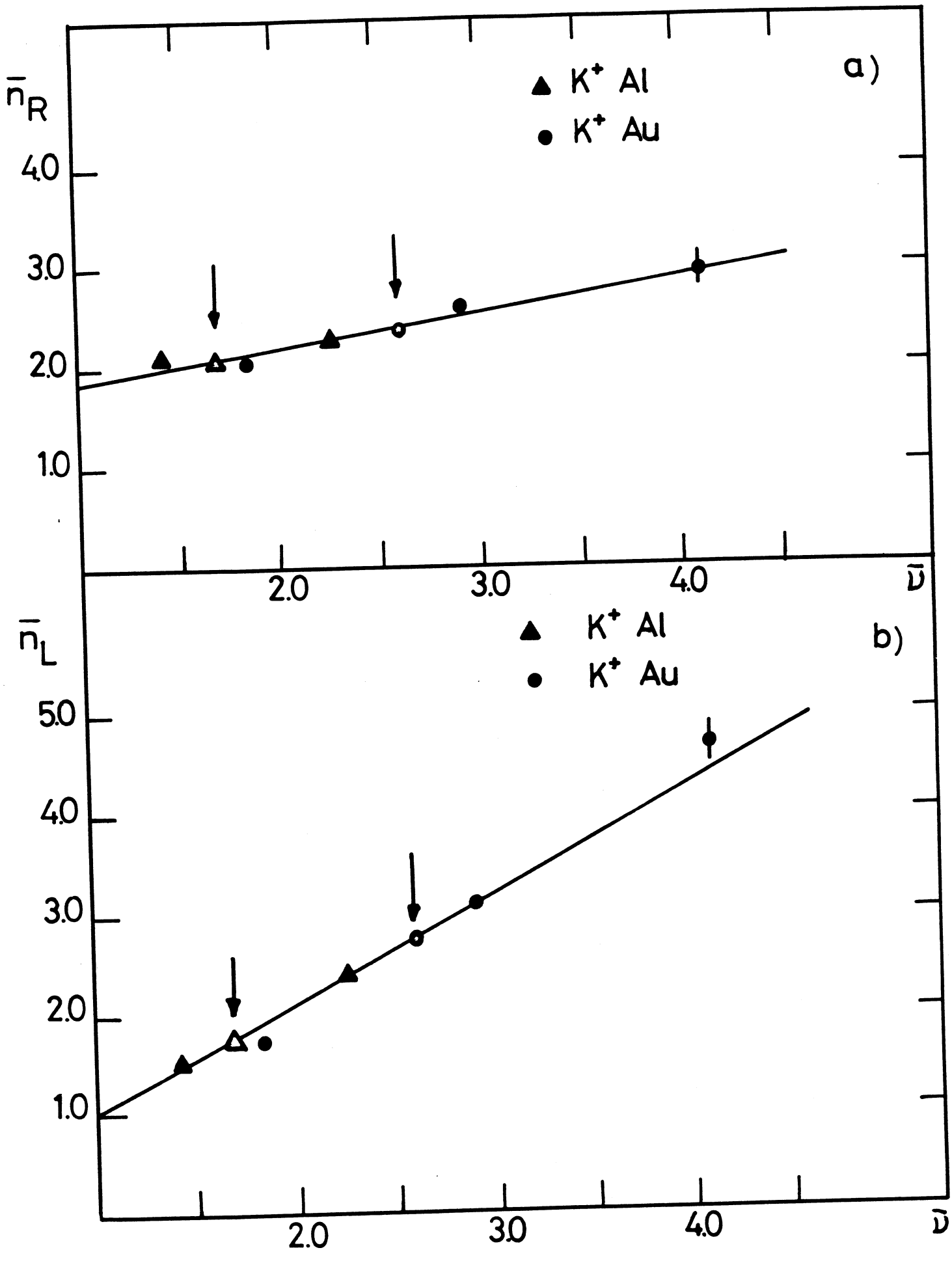
a)
$\bar{n}_R$
▲ K^+ Al
● K^+ Au
4.0
3.0
2.0
1.0
2.0
3.0
4.0
$\bar{\nu}$
b)
$\bar{n}_L$
▲ K^+ Al
● K^+ Au
5.0
4.0
3.0
2.0
1.0
2.0
3.0
4.0
$\bar{\nu}$

FIG. 8